The Journal of Navigation (2024), 1–10
doi:10.1017/S0373463323000255

RESEARCH ARTICLE

Signal design and performance analysis for LEO high dynamic navigation application

Lei Wang,[1] Jibin Che,[2]* and Haoyan Chen[1]

[1] Institute of System Engineering, AMS, Beijing, China
[2] Xidian University, Xi'an, China.
*Corresponding author: Jibin Che; Email: grantche@163.com

Received: 2 May 2022; **Accepted:** 21 October 2023

Keywords: LEO; signal design; high dynamic; CSS; mean acquisition time

Abstract

With the development of GNSS (Global Navigation Satellite System), LEO (Low Earth Orbit) systems are adopted to enhance the system performance of GNSS. The signal Doppler of the LEO satellite is seven to nine times that of GNSS signals, which benefits positioning performance but leads to high acquisition complexity. This paper proposes the combination of a CSS (Chirp Spread Spectrum) marker and the main body of traditional modulation methods for high dynamic application. The acquisition calculation complexity and mean acquisition time of the proposed signal are analysed and compared with the traditional signal. The result shows that the acquisition calculation complexity is just 26 % of the traditional signal under the parameters considered and the mean acquisition time of the proposed signal is also lower than the traditional signal. Hence, the proposed signal is able to decrease the mean acquisition time of the receiver under the constraint of calculation complexity and should be adopted for LEO high dynamic application.

1. Introduction

The LEO (Low Earth Orbit) system is now gaining increasingly more attention. It is of great benefit to satellite navigation and positioning. Enge et al. (2012) analysed the advantage of LEO versus MEO (Medium Earth Orbit). Satellite signals of the LEO system are of much higher signal power than those of MEO satellites for receivers on the ground and this leads to better performance on anti-interference (Iannucci and Humphreys, 2020). The combination of LEO and MEO is able to supply benefits on multipath error degradation and Doppler-based positioning (Jiang et al., 2022). Many researchers have analysed the benefits of LEO on GNSS carrier phase positioning (Joerger, 2009; Li et al., 2022) and the results show that LEO is able to help realise a fast fix of carrier phase cycle ambiguities. Because of the great benefits of LEO, many LEO satellite systems are designed to augment the GNSS (Global Navigation Satellite System) navigation performance, including the Hongyan constellation (Meng et al., 2018) and Luojia-1A satellite (Wang et al., 2018).

In GNSS systems, the signal modulation methods are basically BPSK (Binary Phase Shift Keying), BOC (Binary Offset Carrier), AltBOC (Alternative BOC) and so on (China Satellite Navigation Office, 2023; IS-GPS-200, 2023; IS-GPS-705, 2023; IS-GPS-800, 2023). GNSS receivers must track more than four signals to realise positioning. To track the GNSS signals and decode the information, an acquisition method must first be adopted to detect the presence of the signal. Therefore, acquisition is the first step of GNSS signal processing (Li et al., 2012). To successfully acquire the signal, the receiver has to search for the satellite index, Doppler frequency and time delay. However, LEO satellites are of high

dynamic. The speed of LEO satellites can be as much as 7 Km/s. Therefore, the maximum Doppler of LEO signals can be seven to nine times higher than that of the MEO signals. The receiver has to search in a larger Doppler range to acquire the signal. In addition, the orbital period of LEO satellites is far shorter than that of MEO and this leads to frequent signal acquisition. This leads to high calculation complexity and longer mean acquisition time in signal acquisition if the traditional signal is adopted. Furthermore, the receiver would need more expensive equipment to realise the calculation in real time. Hence, optimisation of the signal for LEO high dynamic application is very necessary to degrade the acquisition calculation complexity and mean acquisition time.

This paper proposes a signal design approach for LEO high dynamic application. It combines CSS (Chirp Spread Spectrum) modulation with traditional signal modulation methods. CSS modulation uses wideband linear frequency modulated pulses to encode information. It is mainly used in radar and satellite based IOT (Internet of Things). It is of high Doppler tolerance, which helps to reduce the acquisition complexity.

The remainder of this paper is organised as follows. First, the model of the proposed signal is introduced. Second, the correlation performance of the proposed signal is analysed to show the acquisition power loss. Third, the calculation complexity of the proposed signal is analysed based on the usual acquisition method. Fourth, the mean acquisition time of the proposed signal is analysed and compared with the traditional navigation signal. Finally, the main topic of the paper is concluded and the future work on this topic is analysed. The analysis results show that the proposed signal is able to decrease the calculation complexity of the receiver compared to the traditional signal. It also decreases the mean acquisition time under the constraint of calculation complexity.

2. Signal model

At the beginning, pseudo random noise code modulated BPSK is adopted for the GPS C/A signal. With the development of other GNSS systems, such as BDS, Galileo and Glonass, the frequency spectrum for satellite navigation becomes increasingly more crowded. Therefore, BOC, AltBOC and similar signal modulation methods are adopted to degrade the cross correlation between signals. The expression of navigation signal based on BPSK and BOC are

$$\begin{aligned} S_{\mathrm{BPSK}}(t) &= AD(t)C(t)\exp(j2\pi f_0 t + \phi_0) \\ S_{\mathrm{BOC}}(t) &= AD(t)SC(t)C(t)\exp(j2\pi f_0 t + \phi_0) \end{aligned} \tag{1}$$

where A is the amplitude, $D(t)$is the navigation message, $C(t)$ is the code, f_0 is the central frequency, ϕ_0 is the initial carrier phase and $\mathrm{SC}(t)$ is the subcarrier of BOC.

Although acquisition method of these kinds of signals is similar, the acquisition calculation complexity of these signals is amplified by the high dynamic of LEO satellites. The proposed signal in this paper is designed to degrade the calculation complexity.

The proposed signal is a combination of CSS signal and traditional signal modulation methods. A CSS signal is used as the signal marker. Traditional signal modulation methods, such as BPSK and BOC, are used as the main body to maintain the performance of multi-access and carrier frequency tracking.

The expression of CSS is (Qian et al., 2019)

$$S_{\mathrm{CSS}}(t) = \begin{cases} \exp\left(j2\pi f_0 t \pm j2\pi\left(\dfrac{\mu t - B}{2}\right)t\right) & 0 \le t < T_s \\ 0 & \text{otherwise} \end{cases} \tag{2}$$

where f_0 is the central frequency, μ is the chirp rate and satisfies $\mu = B/T_s$, T_s is the symbol length, B is the transmission bandwidth, the sign of + makes a positive-chirp signal and − makes a negative-chirp signal.

https://doi.org/10.1017/S0373463323000255 Published online by Cambridge University Press

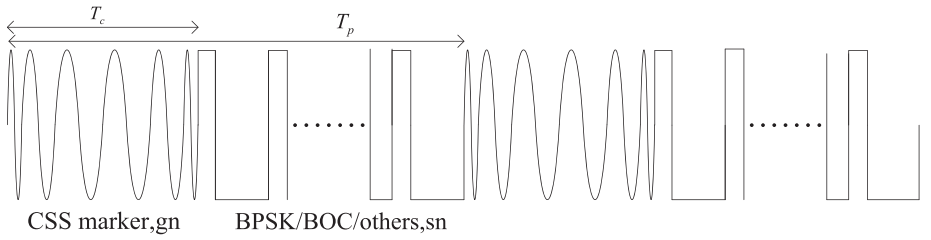

Figure 1. *Structure of the proposed signal.*

The multi-access signal of CSS is limited. Different CSS signals are constructed based on changing the chirp rate (Vangelista, 2017). The performance of orthogonality degrades with the change of chirp rate. It is not enough to allocate one CSS signal for every satellite and maintain the orthogonality performance. Therefore, some work has to be done to design the signal for all the satellites.

The characteristic of the proposed signal is shown as follows.

(1) The signal comprises the CSS marker and main body of a traditional signal. The effective CSS signals are chosen for the markers based on the principle of orthogonality.
(2) The satellite signals will be separated into several groups. The same CSS marker is applied to all the satellites in one group and different groups adopt different CSS marker. The signals in one group should avoid collision based on other multi-access methods such as SDMA (Space Division Multi-Access) or others.

The structure of the proposed signal is shown in Figure 1 and the expression is shown as

$$s(t) = \begin{cases} S_{\mathrm{CSS,gn}}(t - kT_p)e^{j2\pi f_r t} & 0 \le t - kT_p < T_c, k \in \mathrm{N} \\ S_{\mathrm{Main,sn}}(t - kT_p)e^{j2\pi f_r t} & T_c \le t - kT_p < T_p, k \in \mathrm{N} \end{cases} \tag{3}$$

where the subscript gn is the index of group, sn is the index of satellite, f_r is the radio frequency, T_c is the time length of the CSS marker and T_p is the time interval between CSS markers.

Considering that the earliest and most typical navigation signal is based on BPSK (IS-GPS-800, 2023), the main part of the proposed signal is supposed as BPSK in the following. The performance of the proposed signal is analysed and compared with the traditional signal.

3. Correlation functions in acquisition of the proposed signal

The acquisition of navigation signal is the 3-D search of satellite index, time delay and Doppler. For MEO satellites, the maximum signal Doppler of receivers is approximately ±5 KHz. Considering that the relative velocity between the LEO satellite and the receiver can be as large as 7 Km/s, the signal Doppler can be as large as approximately ±37 KHz when the radio frequency is 1575·42 MHz.

For the traditional GPS C/A signal, the code rate is 1·023 Mcps (IS-GPS-800, 2023), and the signal main-lobe bandwidth B_{ml} is two times the code rate. A typical sampling rate in acquisition is two times the code rate and a typical coherent integration time is 1 ms. The signal parameters above are adopted in the following analysis.

In the acquisition of the proposed signal, the local CSS signal correlates with the received signal. Therefore, the receiver obtains the auto-correlation of CSS when the current signal is the CSS marker and the cross-correlation of CSS and BPSK when the current signal is the main body. This part analyses the correlation performance.

https://doi.org/10.1017/S0373463323000255 Published online by Cambridge University Press

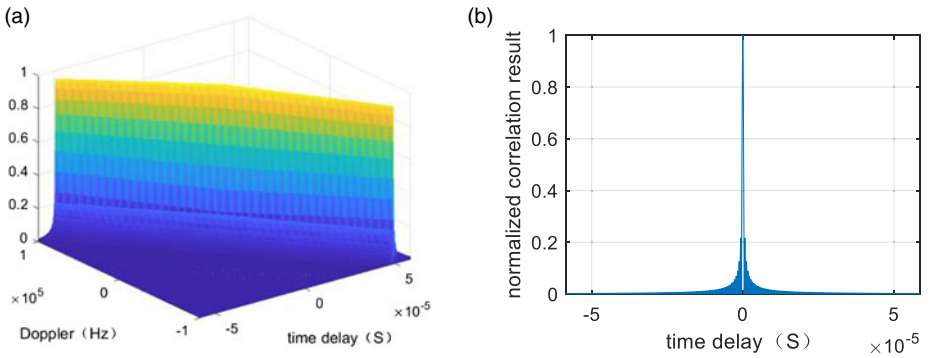

Figure 2. *ACF of CSS. (a) ACF under versus time delay and Doppler, (b) ACF when the Doppler is 0 Hz.*

3.1. Auto-correlation function

The ACF (auto-correlation function) of CSS is shown as follows (Kadlimatti and Fam, 2016):

$$R_{\mathrm{CSS}} = \int_{T_a}^{T_b} e^{\left(j2\pi(f_0+f_e)(t-\tau)+j2\pi\left(\frac{\mu(t-\tau)-B}{2}\right)(t-\tau)\right)}\left(e^{j2\pi f_0 t+j2\pi\left(\frac{\mu t}{2}-B\right)t}\right)^* dt$$
$$= e^{-j\phi}\sin c((f_e-\mu\tau)(T_b-T_a))(T_b-T_a) \tag{4}$$

where f_e is the frequency error, $[T_a, T_b]$ is the integral range, and it satisfies $[T_a, T_b] \subset [0, T]$,$\sin c(x)$ satisfies $\sin c(x) = \sin(\pi x)/\pi x$ and '*' is the conjugate operator in this equation.

When the signal parameters are set as the parameters above, the ACF of CSS under different signal delay and Doppler is shown in Figure 2.

The width of the correlation peak of CSS is $2/B_{\mathrm{ml}}$, which is half the width of BPSK. Additionally, the time delay corresponding to the correlation peak changes with the Doppler.

Therefore, to lower the acquisition power loss, the correlation procedure of the proposed signal should be optimised based on the characteristic of CSS. First, the time delay search interval should be lower than BPSK to reduce the correlation power loss. This can be realised by increasing the sampling rate to two times of BPSK. Second, the signal Doppler should be reverified to obtain the actual time delay and signal Doppler. When searching the actual signal Doppler, the time delay of the local signal should be compensated to get the correlation peak. Suppose that the Doppler to be searched is d_k, the signal should be delayed with d_k/μ. Additionally, the signal can be down sampled by two times to realise the normal sampling rate of BPSK.

When the signal Doppler is 37 KHz, the power loss of the maximum correlation peak is −0·16 dB. Therefore, it is not necessary to implement signal Doppler search when acquiring the CSS marker.

3.2. Cross-correlation function

When the current signal is not the CSS marker, the correlation result should not contain any correlation peak to avoid false alarm. Therefore, this part analyses the cross-correlation function (CCF) of CSS and BPSK. The expression of the cross correlation of local CSS and the received BPSK is shown as (Xie, 2017)

$$R_{\mathrm{CCF}}(\tau, f_d) = \frac{1}{T_s}\int_{-\infty}^{\infty}(S_{\mathrm{BPSK}}(t-\tau)e^{j(2\pi f_d(t-\tau)+\theta_e)})S_{\mathrm{CSS}}(t)dt \tag{5}$$

https://doi.org/10.1017/S0373463323000255 Published online by Cambridge University Press

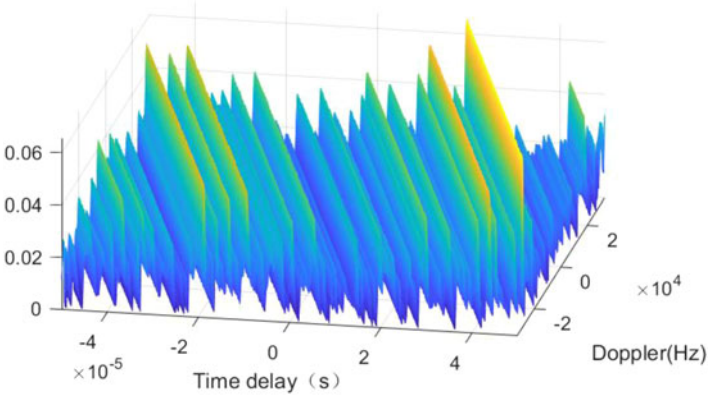

Figure 3. *CCF of CSS and BPSK under different time delay and Doppler.*

The cross correlation depends heavily on the pseudo codes. Therefore, it is analysed based on simulation. The GPS CA codes are adopted for the analysis. The CCF based on different CA codes is analysed and Figure 3 shows an.

The CCF based on different CA code is basically the same. There is no correlation peak in CCF. The maximum correlation peak in the normalised CCF result is 0·0658, which is $-23 \cdot 63$ dB. It is just 0·3 dB higher than the side peak of the CA code, which is $-23 \cdot 94$ dB. The SNR (Signal to Noise Ratio) of the correlation result is usually above 15 dB to realise acceptable detection performance. This means that the CCF peak is far below the noise. Therefore, the CCF peak can be ignored when analysing the false alarm in the following.

3.3. Acquisition procedure

To get the correct signal delay and Doppler, the acquisition of the proposed signal is combined with the acquisition of the CSS marker and the verification based on the main body. Therefore, the procedure of the proposed signal is shown as follows.

Step 1. Correlate the CSS local signal with the received signal. Determine whether the CSS marker is acquired. If it is not acquired, go back to the correlation with the received signal.
Step 2. If the CSS marker is acquired, correlate the corresponding local BPSK signal with the received signal to obtain the satellite index and signal Doppler. If the signal Doppler is not acquired correctly, the receiver goes to Step 1.
Step 3. If the signal is acquired correctly based on Step 2, the acquisition ends and the receiver turns to signal tracking.

Therefore, the calculation complexity and the mean acquisition time of the proposed signal should be analysed based on the acquisition procedure.

4. Calculation complexity

The acquisition calculation complexity determines the resources that the receiver needs. For example, if the signal processing equipment is a CPU (Central Processing Unit), when the calculation complexity increases, the receiver will be unable to realise real-time acquisition of the signals with the same CPU. Therefore, calculation complexity is an important index of the signal performance. This part analyses the calculation complexity of the proposed signal.

Suppose that the receiver adopts a time parallel correlation algorithm for signal correlation. The following symbols are adopted in the paper. Here, N_s is the number of the signal samples, N_{FFT} is the

https://doi.org/10.1017/S0373463323000255 Published online by Cambridge University Press

number of FFT points, N_f is the number of frequency search interval, N_{grpn} is the number of satellites in one group and N_T is the rate of T_p to T_c. When the sampling rate of CSS is two times BPSK, N_s and N_{FFT} satisfy$N_{\text{FFT}} = 2 \times \text{next2pow}(N_s)$, $N_{s,\text{CSS}} = 2N_{s,\text{BPSK}}$ and $N_{\text{FFT,CSS}} = 2N_{\text{FFT,BPSK}}$.

The calculation complexity of CSS correlation is obtained based on the calculation complexity of the time parallel correlation algorithm (Zhu and Fan, 2015). It is combined with two times $N_{\text{FFT,CSS}}$ point complex FFT, one $N_{\text{FFT,CSS}}$ point complex multiplication and one $N_{\text{FFT,CSS}}$ point complex IFFT. Therefore, the total calculation complexity is

$$\begin{aligned} \text{Multiplication}: O_{M,\text{CSS}} &= O_{M,\text{FFT,CSS}} \times 2 + O_{M,\text{IFFT,CSS}} + O_{M,\text{cor,CSS}} \\ &= 2N_{\text{FFT,CSS}}\log_2(N_{\text{FFT,CSS}}) \times 3 + 4N_{\text{FFT,CSS}} \end{aligned} \tag{6}$$

$$\begin{aligned} \text{Addition}: O_{A,\text{CSS}} &= O_{A,\text{FFT,CSS}} \times 2 + O_{A,\text{IFFT,CSS}} + O_{A,\text{cor,CSS}} \\ &= 3N_{\text{FFT,CSS}}\log_2(N_{\text{FFT,CSS}}) \times 3 + 2N_{\text{FFT,CSS}} \end{aligned} \tag{7}$$

where O is used as the expression of calculation complexity.

During the signal reverification, N_f signal Doppler search and three code phase search are necessary to control the power loss. Therefore, the calculation complexity for satellite index search and Doppler acquisition is composed of $(N_{\text{grpn}} \times N_f \times 3)$ times $N_{s,\text{BPSK}}$ point complex multiplication. It is shown as

$$\begin{aligned} \text{Multiplication}: O_{M,DpAq} &= O_{M,\text{commul}} \times N_{\text{grpn}} \times N_f \times 3 \\ &= 4N_{s,\text{BPSK}} \times N_{\text{grpn}} \times N_f \times 3 \end{aligned} \tag{8}$$

$$\begin{aligned} \text{Addition}: O_{A,DpAq} &= O_{A,\text{cor}} \times N_{\text{grpn}} \times N_f \times 3 \\ &= 2N_{s,\text{BPSK}} \times N_{\text{grpn}} \times N_f \times 3 \end{aligned} \tag{9}$$

where $O_{M,\text{commul}}$ is the calculation complexity of $N_{s,\text{BPSK}}$ point complex multiplication.

Considering that the location of the correct CSS marker is random during the signal length T_p, the average number of CSS correlation is $N_T/2$, which means that the average calculation complexity of the proposed signal for one satellite is

$$\text{Multiplication}: O_{M,\text{PS}} = \left(\begin{array}{l} (2N_{\text{FFT,CSS}}\log_2(N_{\text{FFT,CSS}}) \times 3 + 4N_{\text{FFT,CSS}}) \times N_T/2 \\ +4N_{s,\text{BPSK}} \times N_{\text{grpn}} \times N_f \times 3 \end{array} \right) / N_{\text{grpn}} \tag{10}$$

$$\text{Addition}: O_{A,\text{PS}} = \left(\begin{array}{l} (3N_{\text{FFT,CSS}}\log_2(N_{\text{FFT,CSS}}) \times 3 + 2N_{\text{FFT,CSS}}) \times N_T/2 \\ +2N_{s,\text{BPSK}} \times N_{\text{grpn}} \times N_f \times 3 \end{array} \right) / N_{\text{grpn}} \tag{11}$$

The acquisition calculation complexity of the BPSK signal comprises $(N_f + 1)$ times$N_{\text{FFT,BPSK}}$ point FFT, one $N_{s,\text{BPSK}}$ point complex multiplication, N_f times $N_{\text{FFT,BPSK}}$ point complex multiplication and one $N_{\text{FFT,BPSK}}$ point IFFT. It is shown as

$$\text{Multiplication}: O_{M,\text{BPSK}} = \left(\begin{array}{l} 2(N_f + 2)N_{\text{FFT,BPSK}}\log_2(N_{\text{FFT,BPSK}}) \\ + 4N_f N_{\text{FFT,BPSK}} + 4N_{s,\text{BPSK}} \end{array} \right) \tag{12}$$

$$\text{Addition}: O_{A,\text{BPSK}} = \left(\begin{array}{l} 3(N_f + 2)N_{\text{FFT,BPSK}}\log_2(N_{\text{FFT,BPSK}}) \\ +4N_f N_{\text{FFT,BPSK}} + 2N_{s,\text{BPSK}} \end{array} \right) \tag{13}$$

For calculators, the resource needed for multiplication is less than that of addition. Therefore, the calculation complexity of multiplication is mainly considered and it is shown in Figure 4.

From the above analysis, the following conclusions are obtained.

(1) The average calculation complexity of the proposed signal increases with the increment of N_T and the decrement of N_{grpn}.

https://doi.org/10.1017/S0373463323000255 Published online by Cambridge University Press

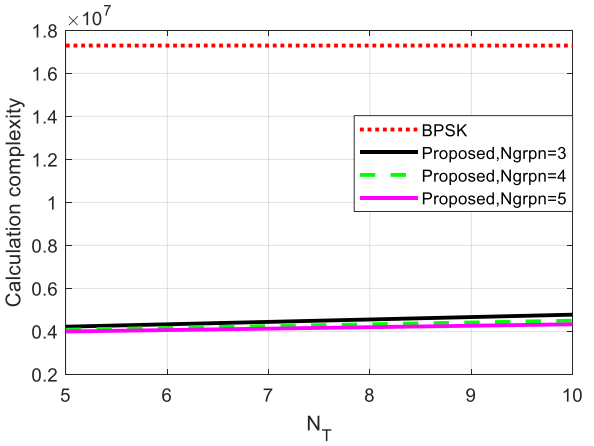

Figure 4. *Calculation complexity versus* N_T.

(2) The average calculation complexity of the proposed signal for one satellite is basically lower than that of BPSK. When N_{grpn} is 4 and N_T is 10, the average calculation complexity of the proposed signal is just 26 % of that of BPSK.

Therefore, the proposed signal is able to decrease the calculation complexity of the receiver compared to the traditional signal.

5. Mean acquisition time

Mean acquisition time (MAT) shows the time to successfully acquire the signal for the receiver. This part compares the MAT of the receiver when the other parameters are constraint as the same.

5.1. Expression of the MAT

Park et al. (2002) analysed the expression of the MAT based on the statistical model. The expression is

$$\begin{aligned} T_{M,\text{BPSK}} = {} & (\bar{N}_C - 1)T_D(1 + k_p(1 - (1 - P_f)^{M_p})) \left(\frac{2 - P_D}{P_D}\right) \\ & + \frac{T_D}{P_D}(1 + k_p(1 - (1 - P_f)^{M_p - 1})) \end{aligned} \tag{14}$$

where $\bar{N}_C$ is the number of search blocks, T_D is the dwell time for single search block, P_D is the probability of detection for single detection, T_f is the penalty time for false alarm, k_p is the penalty coefficient ($T_f = k_p T_D$), M_p is the number of parallel search cell and P_f is the probability of false alarm.

The penalty time of BPSK is basically T_D, because the receiver is able to carry out another correlation to verify the acquisition result during the dwell time.

The MAT of the CSS marker is comparable to the expression above. For the proposed signal, the number of search blocks is the number of the possible positions of the CSS marker in one signal period, which is N_T. The number of search cells in each search block is two times that of BPSK. The false alarm penalty time is equal to the time of signal Doppler acquisition. The MAT of the proposed signal contains the time of signal Doppler acquisition based on the MAT of CSS marker. Therefore, the MAT

https://doi.org/10.1017/S0373463323000255 Published online by Cambridge University Press

of the proposed signal is

$$T_{M,\text{proposed}} = \left(\begin{array}{l} (N_T - 1)T_D(1 + k_{p,\text{pro}}(1 - (1 - P_f)^{M_{p,\text{CSS}}})) \left(\dfrac{2 - P_{D,\text{CSS}}}{P_{D,\text{CSS}}} \right) \\ + \dfrac{T_D}{P_{D,\text{CSS}}}(1 + k_{p,\text{pro}}(1 - (1 - P_f)^{M_{p,\text{CSS}}-1})) + k_{p,\text{pro}}T_D \end{array} \right) \tag{15}$$

The value of $k_{p,\text{pro}}$ can be expressed as $k_{p,\text{pro}} = \lceil N_{\text{grpn}} \times N_f \times 3/N_{\text{mp}} \rceil$. The penalty time is the dwell time to deal with the calculation during the Doppler acquisition. In software receivers, the processing time is determined by the calculation complexity. Considering that the maximum calculation complexity is the CSS correlation, the processing procedures that are of lower calculation complexity are also able to be solved in the dwell time T_D. Therefore, the maximum number of parallel correlations satisfies

$$N_{\text{mp}} = \lfloor (O_{M,\text{FFT,CSS}} + O_{M,\text{IFFT,CSS}} + O_{M,\text{cor,CSS}})/O_{M,\text{cor}} \rfloor \tag{16}$$

and $\lfloor x \rfloor$ and $\lceil x \rceil$ are separately the floor integer and the ceiling integer. The $O_{M,\text{FFT,CSS}}$ of the local signal is ignored because it can be restored in advance instead of calculating in real time.

Identically, when comparing the MAT of the traditional BPSK signal and that of the proposed signal, the calculation complexity is also considered. The maximum number of parallel search blocks in T_D satisfies the following expression:

$$N_{\text{mb}} = \left\lfloor \left(\begin{array}{l} O_{M,\text{FFT,CSS}} + O_{M,\text{IFFT,CSS}} \\ + O_{M,\text{cor,CSS}} - O_{M,\text{FFT,BPSK}} \end{array} \right) / (O_{M,\text{IFFT,BPSK}} + O_{M,\text{cor,BPSK}}) \right\rfloor \tag{17}$$

and the number of search blocks is $\bar{N}_c = \lceil N_f / N_{\text{mb}} \rceil$.

5.2. Results of MAT

The probability of detection has to be obtained to get the MAT. When using a square-law detector, the probability of detection is expressed as follows (Liu et al., 2019):

$$\begin{aligned} \lambda &= \sum_{i=1}^{N_{ncoh}} (m_I^2(i|H_1) + m_Q^2(i|H_1)) = 2 \sum_{i=0}^{N_{ncoh}-1} \text{SNR}_i \\ &= 2D_{\text{DS}} \sum_{i=0}^{N_{ncoh}-1} D(f_d, f_a, f_c, T_c, i) C N_0 \cdot T_{coh} \end{aligned} \tag{18}$$

where D_{DS} is the front-end power loss of the receiver, $D(f_d, f_a, f_c, T_c, i)$ is the correlation loss, CN_0 is the Carrier to Noise power spectral density Ratio (CNR), T_{coh} is the coherent integration time length, N_{ncoh} is the times of the non-coherent accumulation and SNR_i is the signal to noise rate for the ith non-coherent integration.

Suppose that D_{DS} is identical for the proposed signal and BPSK. From the results of Section 3.1, it can be obtained that the maximum correlation loss of CSS is $-1 \cdot 04$ dB when the Doppler is 37 KHz and the sampling rate is $2\,B_{\text{ml}}$, while the Doppler loss and the code phase loss are separately $-0 \cdot 91$ dB and $-1 \cdot 16$ dB for the traditional BPSK signal.

Suppose that P_f is 1×10^{-6}, then the probability of detection versus CNR and the MAT versus CNR is shown in Figures 5 and 6.

From the above analysis, the following conclusions are obtained.

(1) The probability of detection of the proposed signal is higher than the traditional BPSK for the same CNR because of the correlation loss advantage.

https://doi.org/10.1017/S0373463323000255 Published online by Cambridge University Press

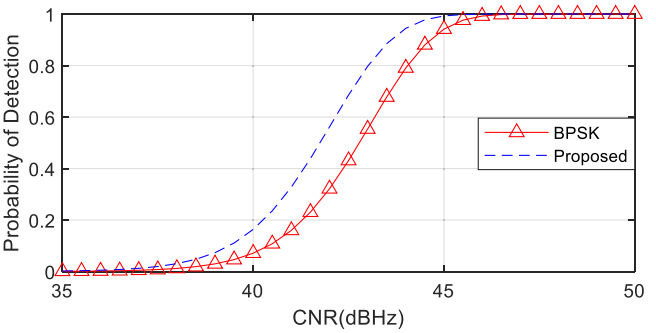

Figure 5. *Probability of detection versus CNR.*

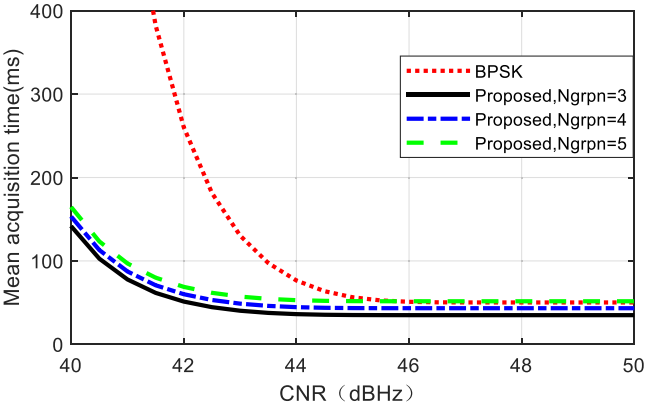

Figure 6. *MAT of BPSK and CSS versus CNR.*

(2) The MAT of the proposed signal increases with the increment of N_{grpn}. This is because the increment of N_{grpn} leads to the increment of false alarm penalty time. When N_{grpn} is 5, the MAT of the proposed signal is higher than that of BPSK when the CNR is higher than 46 dBHz.
(3) The advantage of the proposed signal is greater when the CNR is lower than 45 dBHz. This is mainly determined by the advantage of probability of detection. When N_{grpn} is 4 and the CNR is 45 dBHz, the MAT of the proposed signal is just 91·8 % of the MAT of BPSK.

Therefore, the proposed signal is able to decrease the mean acquisition time of the receiver under the constraint of calculation complexity.

6. Conclusion

This paper proposes the signal comprising the CSS marker and the main body of traditional signal, and satellites are set into groups based on CSS markers. The analysis reveals that the proposed signal shows better performance on acquisition calculation complexity and mean acquisition time compared with the traditional signal. The results show that the average calculation complexity is determined by the number of satellites in one group and CSS marker interpolation ratio. When the two parameters are separately 4 and 10, the average calculation complexity of the proposed signal is just 26 % that of BPSK. The mean acquisition time of the proposed signal is also lower than that of BPSK. When the number of satellites in one group is four and the CNR is 45 dBHz, the MAT of the proposed signal is just 91·8 % that of BPSK. Therefore, it is advantageous for LEO high dynamic application.

The proposed signal will decrease the mean acquisition time of the receiver under the constraint of calculation complexity. Our study recommends its adoption for LEO high dynamic application subject to the tracking performance, which is the focus of our future work.

https://doi.org/10.1017/S0373463323000255 Published online by Cambridge University Press

References

China Satellite Navigation Office. (2023). BeiDou Navigation Satellite System Open Service Performance Standard. Available at https://www.beidou.gov.cn (accessed January 2023).

Enge, P., Bart, F., Jeff, B., David, W., Greg, G. and David, L. (2012). Orbital Diversity for Satellite Navigation. *Proceedings of the 25th International Technical Meeting of the Satellite Division of the Institute of Navigation*, Nashville, TN, 3834–3846.

Iannucci, P. A. and Humphreys, T. E. (2020). Economical Fused LEO GNSS. *2020 IEEE/ION Position, Location and Navigation Symposium (PLANS)*, 426–443.

IS-GPS-200. (2023). NAVSTAR GPS Space Segment/Navigation User Segment Interfaces. Available at https://www.gps.gov (accessed January 2023).

IS-GPS-705 (2023). Navstar GPS Space Segment/ User Segment L5 Interfaces. Available at https://www.gps.gov (accessed January 2023).

IS-GPS-800 (2023). NAVSTAR GPS Space Segment/ User Segment L1C Interfaces. Available at https://www.gps.gov (accessed January 2023).

Jiang, M. Y., Qin, H. L., Zhao, C. and Sun, G. Y. (2022). LEO Doppler-aided GNSS position estimation. *GPS Solutions*, **26**, 31–48.

Joerger, M. (2009). Carrier Phase GPS Augmentation using Laser Scanners and using Low Earth Orbiting Satellites. Dissertations, Illinois Institute of Technology. Chicago.

Kadlimatti, R. and Fam, A. T. (2016). Doppler Detection for Linear FM Waveform Using Extended Matched Filter. *IEEE Radar Conference*, Philadelphia, PA.

Li, H., Li, Y., Peng, W. and Wen, B. (2012). A Novel algorithm for the weak GPS signals acquisition. *The 2nd International Conference on Computer Application and System Modeling*, 738–741.

Li, M., Xu, T., Guan, M., Gao, F. and Jiang, N. (2022). Leo-constellation-augmented multi-GNSS real-time PPP for rapid re-convergence in harsh environments. *GPS Solutions*, **26**(1), 1–12.

Liu, Q., Kou, Y., Huang, Z., Wang, J. and Yao, Y. (2019). Mean acquisition time analysis for GNSS parallel and hybrid search strategies. *GPS Solutions*, **23**(94), 94–107.

Meng, Y., Bian, L., Han, L., Lei, W. Y., Yan, T., He, M. and Li, X. X. (2018). A Global Navigation Augmentation System Based on LEO Communication Constellation. *2018 European Navigation Conference*, Gothenburg.

Park, S. H., Choi, I. H., Lee, S. J. and Kim, Y. B. (2002). A Novel GPS Initial Synchronization Scheme Using Decomposed Differential Matched Filter. *Proceedings of the 2002 National Technical Meeting of The Institute of Navigation*. San Diego, CA: ION, 246–253.

Qian, Y., Ma, L. and Liang, X. (2019). The acquisition method of symmetry chirp signal used in LEO satellite internet of things. *IEEE Communications Letters*, **23**(9), 1572–1575.

Vangelista, L. (2017). Frequency shift chirp modulation: The lora modulation. *IEEE Signal Processing Letters*, **24**(12), 1818–1821.

Wang, L., Chen, R., Li, D., Zhang, G., Shen, X., Yu, B. G., Wu, C. L., Xie, S., Zhang, P., Li, M. and Pan, Y. J. (2018). Initial assessment of the LEO based navigation signal augmentation system from luojia-1A satellite. *Sensors*, **18**, 3919–3938.

Xie, G. (2017). *Principles of GPS and Receiver Design*. Beijing, China: Publishing House of Electronics Industry.

Zhu, C. and Fan, X. (2015). A novel method to extend coherent integration for weak GPS signal acquisition. *IEEE Communications Letters*, **19**(8), 1343–1346.

Cite this article: Wang L, Che J, Chen H (2024). Signal design and performance analysis for LEO high dynamic navigation application. *The Journal of Navigation* 1–10. https://doi.org/10.1017/S0373463323000255